Pressure-induced phase transitions in new luminescent gold(I)-arylacetylide – Supporting Information

Róża Dziewiątkowska[a], Joanna Krzeszczakowska[a], Marta Głodek[b], Michał Łomzik[b], Damian Plażuk[b,c] and Anna Makal[a]

[a] *Chemistry Department, Biological and Chemical Research Centre, University of Warsaw, ul. Żwirki i Wigury 101, 02-089 Warszawa, Poland*
[b] *Department of Organic Chemistry, Faculty of Chemistry, University of Łódź, Tamka 12, 91-403 Łódź, Poland*
[c] *Laboratory of Molecular Spectroscopy, Faculty of Chemistry, University of Łódź, Tamka 12, 91-403 Łódź, Poland*

Contents

S1 Preliminary analysis

S1.1 NMR spectra

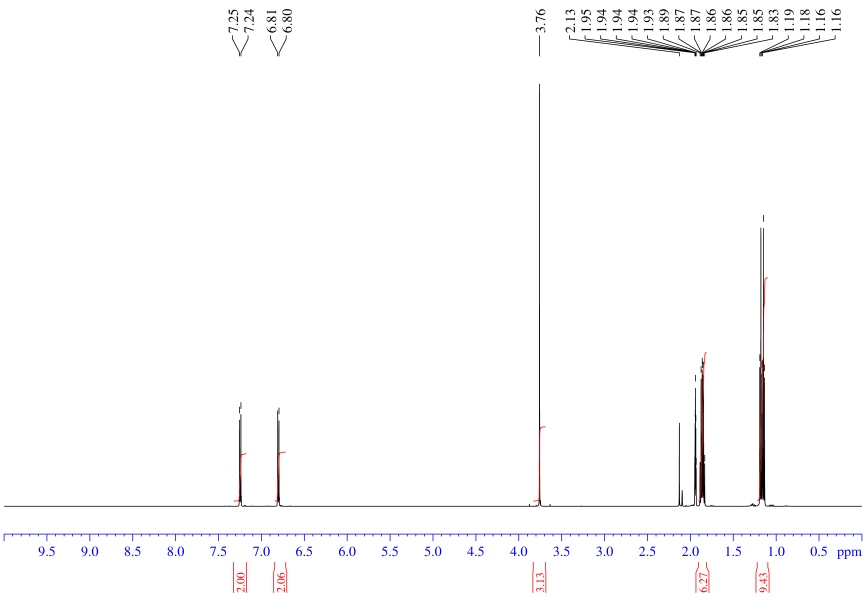

Figure S1.1: ^{1}H NMR spectrum for **ArPEt** in CD_3CN.

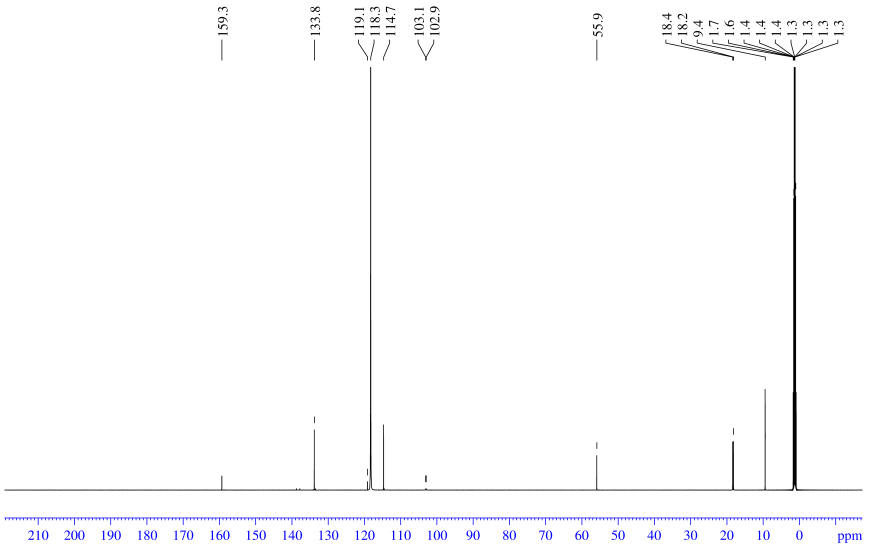

Figure S1.2: $^{13}C\{^{1}H\}$ NMR spectrum for **ArPEt** in CD_3CN.

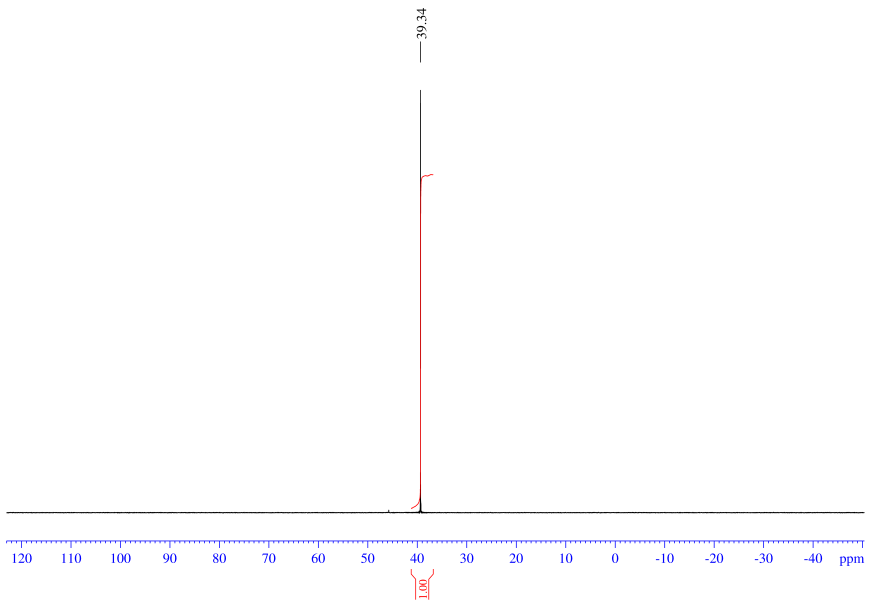

Figure S1.3: $^{31}P\{^{1}H\}$ NMR spectrum for **ArPEt** in CD_3CN.

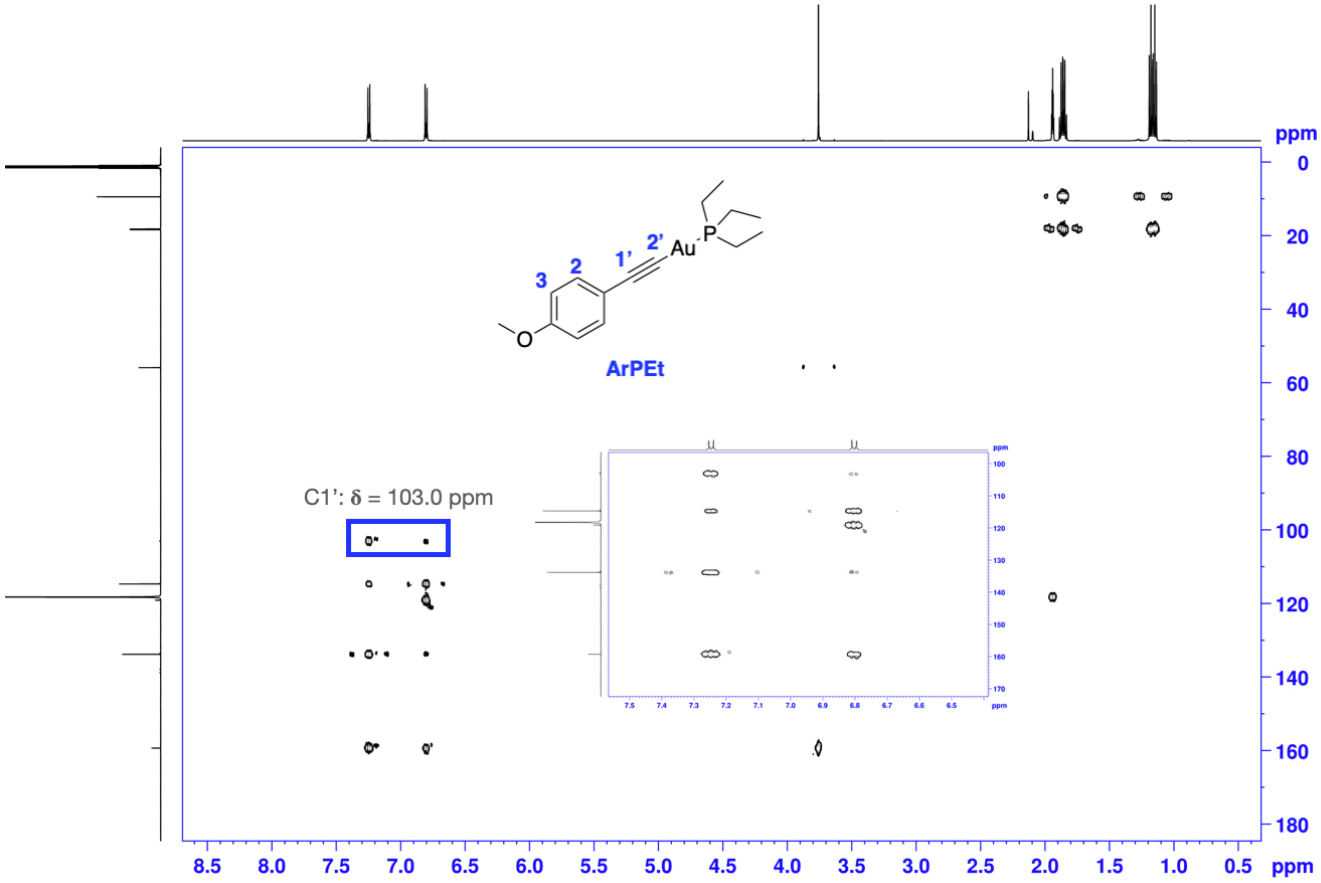

Figure S1.4: ^{1}H-^{13}C HMBC NMR spectrum for **ArPEt** in CD_3CN.

S1.2 Mass spectrometry (MS) data

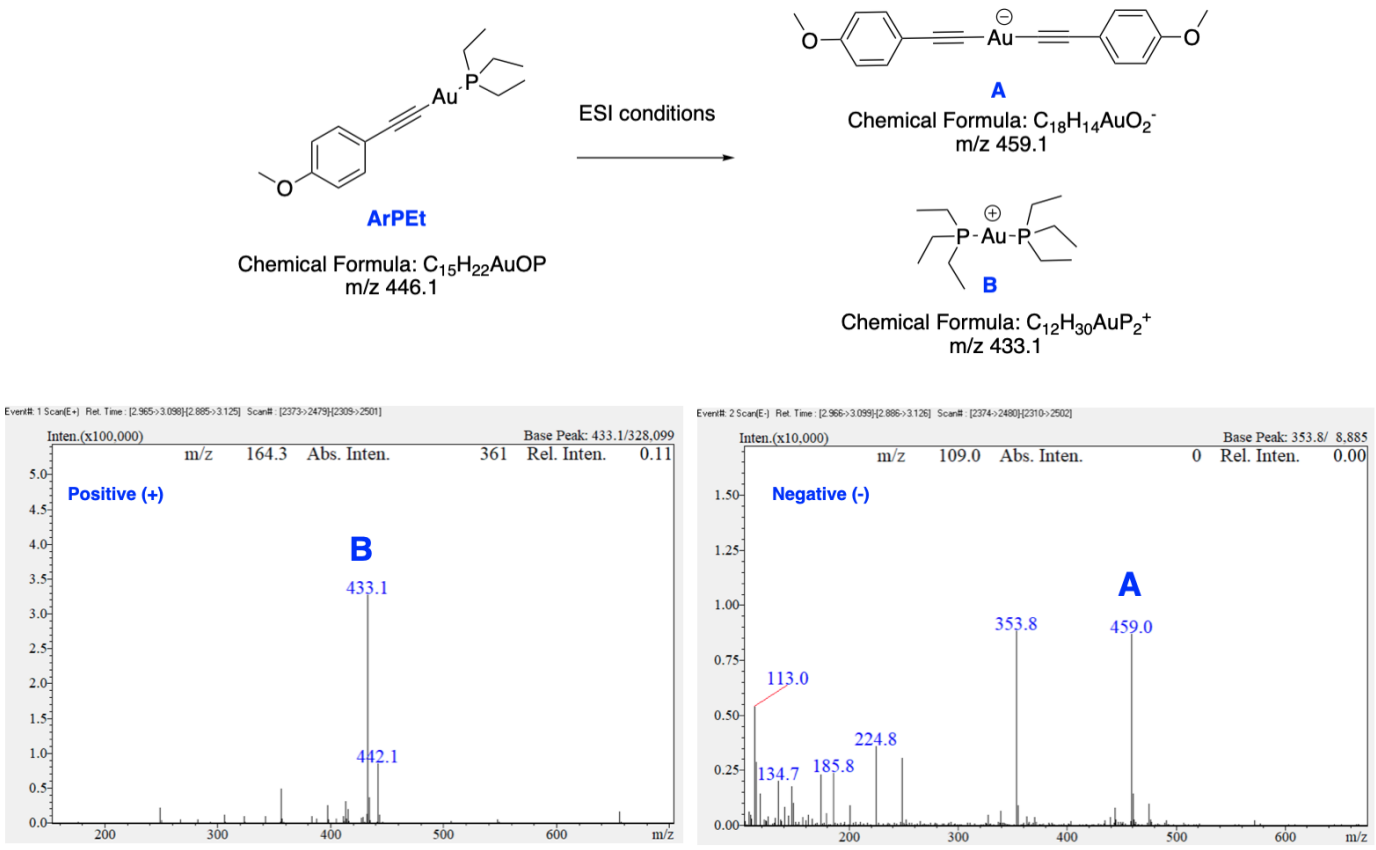

Figure S1.5: ESI-MS analysis for **ArPEt**.

S1.3 Differential Scanning Calorimetry

The DSC measurements were performed using Mettler-Toledo DSC1 STAR^e system at a cooling/heating rate of 10°C/min under a dry N_2 atmosphere and at a constant flow (60 ml/min) first cooling the sample from 22 to -150°C, then warming it back to 22°C and finally heating it to 100°C. Obtained data were analyzed using the STARe software provided by Mettler Toledo. The total of 10.12 mg was accurately weighted into open standard 40 μl aluminum crucible using Mettler-Toledo XS105 DualRange balance. The results of DSC measurements of ArPEt depicted in Figure S1.6. The major endothermic peak at the 87.34 represents the melting point, with the enthalpy of this transition at 36.3 J/g. The minor endo- and exothermic features on cooling, noticeable at 5.75°C and -117.71°C indicate structure reorganizations which will be subject to a separate publication.

Melting point was also redetermined using the MP70 Melting Point System capillary apparatus (Mettler Toledo) with a heating rate of 10°C/min, yielding result within 1°C of the observation from DSC approach.

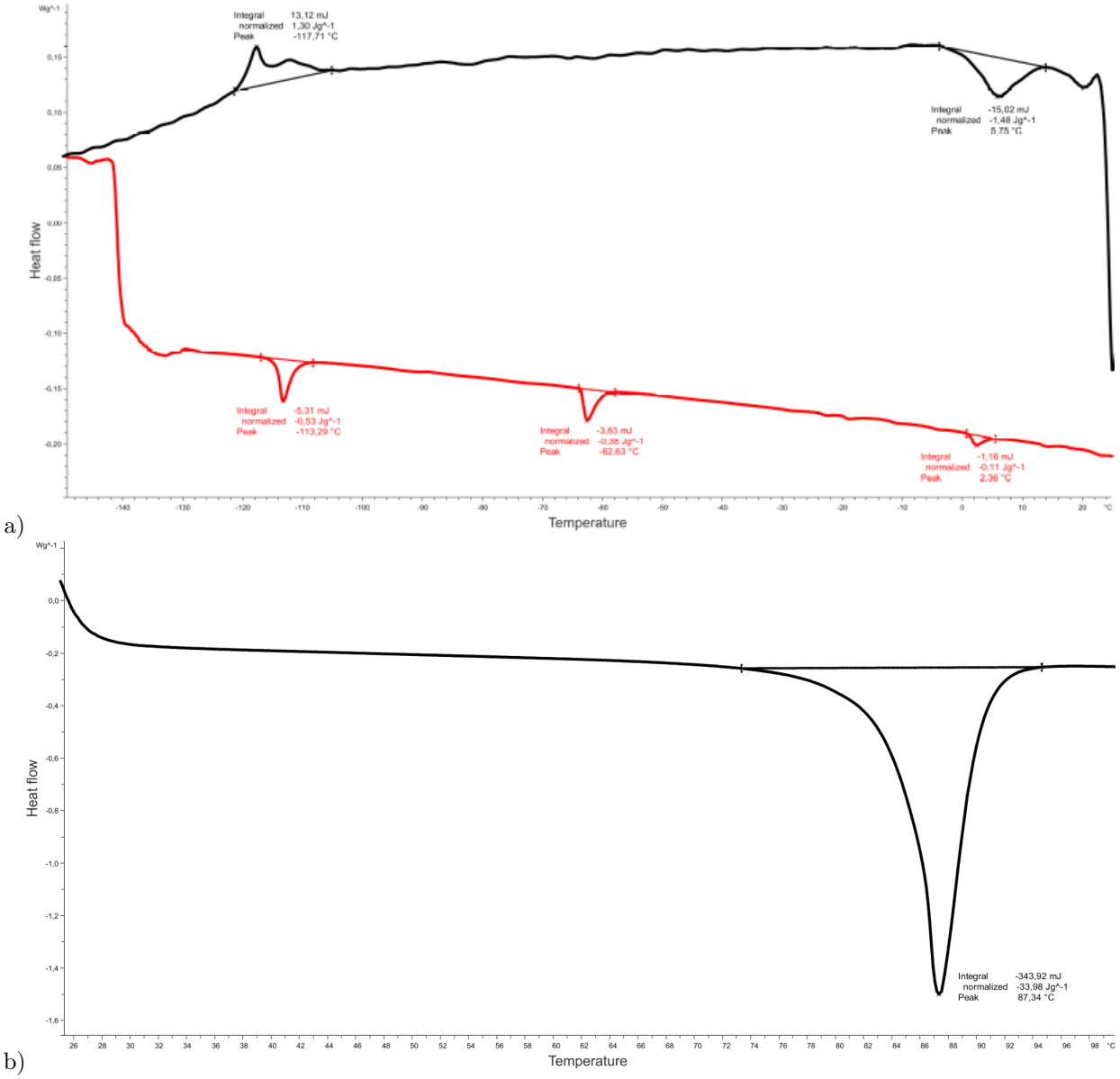

Figure S1.6: Results of DSC measurement of ArPEt: a) black line - cooling, red line heating, b) heating up to the melting point

S2 X-ray diffraction experiments

S2.1 Loading Diamond Anvil Cell

S2.1.1 Procedure

Crystal orientation in DAC is very important to achieve best possible completeness of high-pressure diffraction data, inherently incomplete due to the sample holder. As shown in the work of Tchon et. al.[Tchoń and Makal(2021)], proper orientation, fully utilizing the crystal symmetry, can increase achievable data completeness almost 2-fold.

In order to orient a crystal, a following procedure was executed. Firstly, a short diffraction 'pre-experiment' was performed and a movie recorded in order to match crystal faces with crystallographic directions. Initial experiments were done at 295 K for series 1 (appr2), 3 (appr5) 4 (appr6) and at 100 K for series 2 (appr 4). Appropriate orientation (allowing to achieve better completeness with possibility of systematic extinction analysis) was determined based on potency maps [Tchoń and Makal(2021)] (see next subsection).

In order to orient specific crystal faces with respect to the DAC axis, a crystal was than affixed to a dried drop of epoxy glue placed in the center of diamond cullet. It is important to use as little amount of glue as possible needed to immobilize crystal in DAC.

S2.1.2 Potency maps

A potency map shows completeness of high-pressure diffraction data (in %) possible to achieve with a given radiation wavelength, a DAC opening angle and a point group of the crystal as a function of the crystal orientation in a DAC (i.e. the relative position of crystallographic directions with respect to the vector normal to the diamond culets). It indicates the range of the most convenient orientations of a crystal prior to its placement, but also allows to determine how much data can be collected from an already mounted sample by marking its particular orientation as a point on the map.

Potency maps used in this work (Figures S2.7 – S2.11) were calculated using Python script written by Daniel Tchoń [Tchoń and Makal(2021)]. Crystallographic directions in figures are consistent with the conventional $Pbca$, $Pca2_1$ and Pc unit cell settings – differently than it was chosen in the article ($Pbca$, $Pb2_1a$ and $P11a$). The actually achieved orientations for each crystal were marked with black squares.

Without sample orienting, crystals tend to lay on their main faces, which would usually result in one of the crystallographic directions being aligned with the vector normal to the diamond culet and consequently in minimal or close to minimal potency. It is clearly visible in case of series 2 (appr4, Figure S2.8), where crystal was not properly glued and moved during closing DAC and increasing pressure. Resulting potency is much lower than "average" (mean value in idealized situation, when crystal is spherical) potency.

Interestingly, potency value close to average was achieved as the mean of values for four crystal specimens from synchrotron measurements. Those specimens derived from bigger crystals which were cut into small pieces.

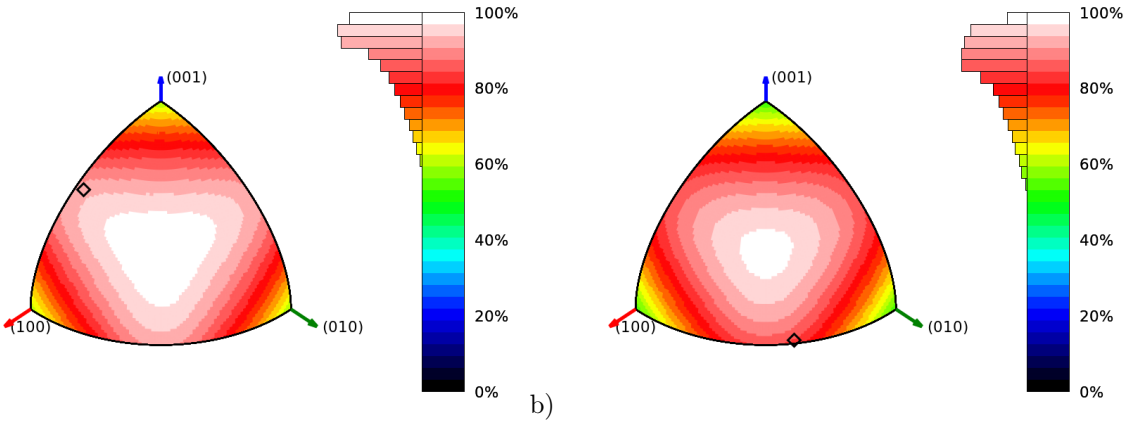

Figure S2.7: Potency maps for chosen pressure points before and after first phase transition for series 1:
a) appr2_0p26GPa, potency: 0.9234 (min: 0.5896, max: 0.9969, average: 0.8836),
b) appr2_0p89GPa, potency: 0.8372 (min: 0.5207, max: 0.9826, average: 0.8417).
Directions on graph b) are consistent with $Pca2_1$ space group instead of $Pb2_1a$ space group.

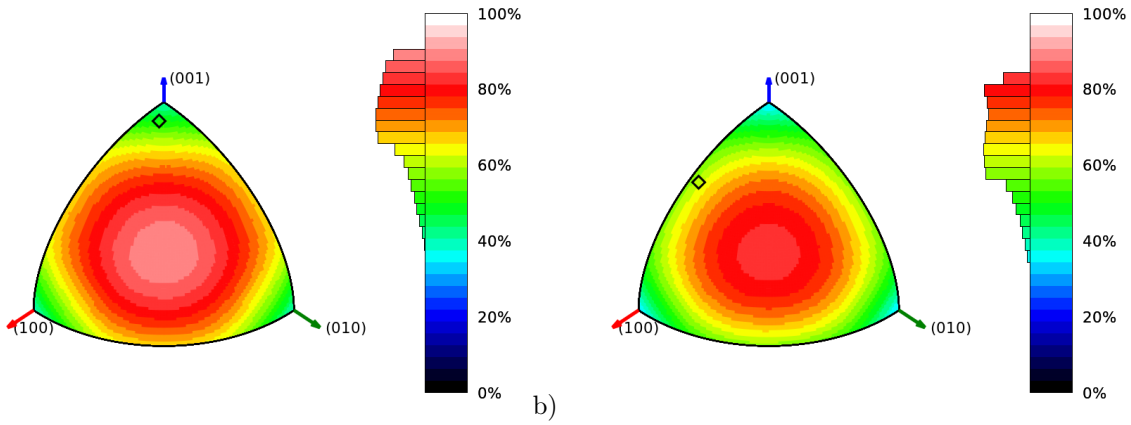

Figure S2.8: Potency maps for chosen pressure points for series 2:
a) appr4_0p16GPa, potency: 0.4963 (min: 0.3800, max: 0.9024, average: 0.7251),
b) appr4_0p45GPa, potency: 0.6102 (min: 0.3257, max: 0.8305, average: 0.6605).
Crystal was not properly glued and moved in DAC during closing it and with increasing pressure.

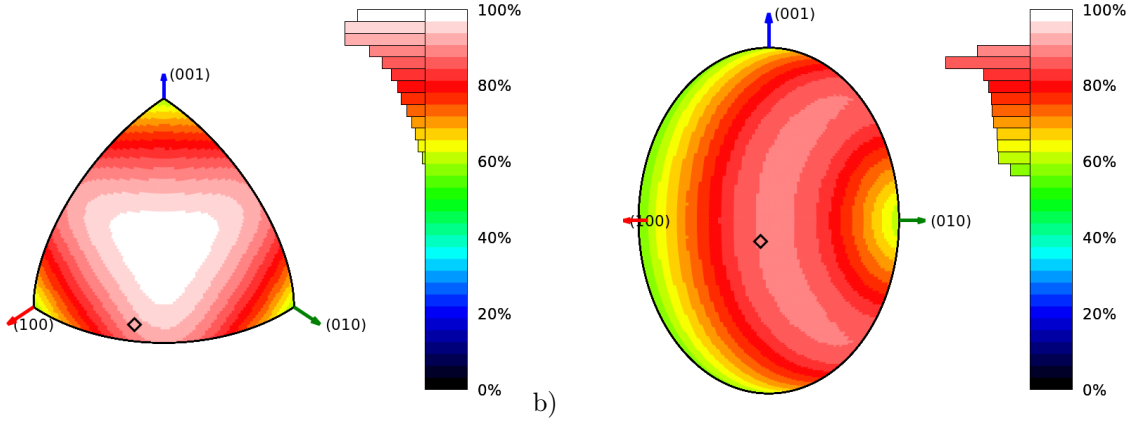

Figure S2.9: Potency maps for chosen pressure points (beginning and final) for series 3:
a) appr5_0p33GPa, potency: 0.9169 (min: 0.5783, max: 0.9966, average: 0.8795),
b) appr5_2p13GPa, potency: 0.8764 (min: 0.5704, max: 0.8845, average: 0.7639).
Directions on graph b) are consistent with Pc space group instead of $P11a$ space group.

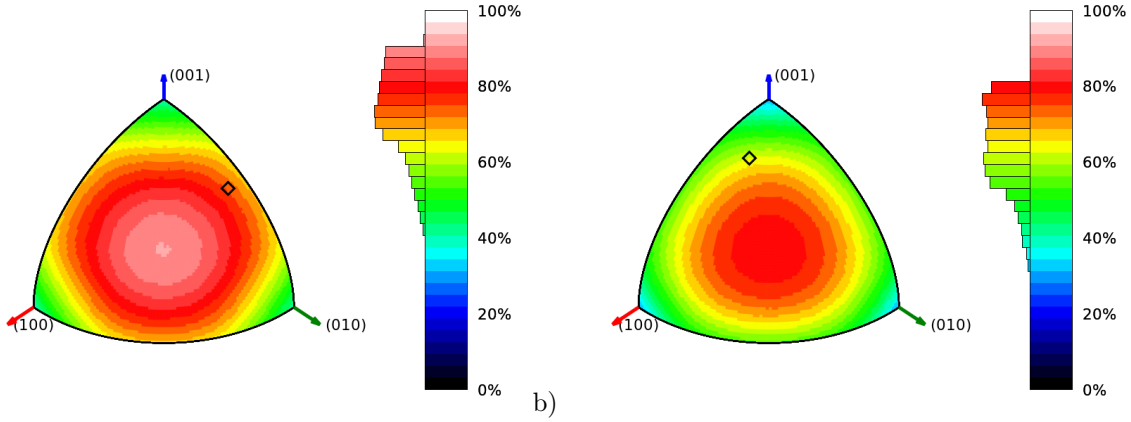

Figure S2.10: Potency maps for chosen pressure points before and after second phase transition for series 4:
a) appr6_0p94GPa, potency: 0.7459 (min: 0.3715, max: 0.9085, average: 0.7336),
b) appr6_2p59GPa, potency: 0.6216 (min: 0.3023, max: 0.8063, average: 0.6388).
Directions on graph b) are consistent with $Pca2_1$ space group instead of $Pb2_1a$ space group.

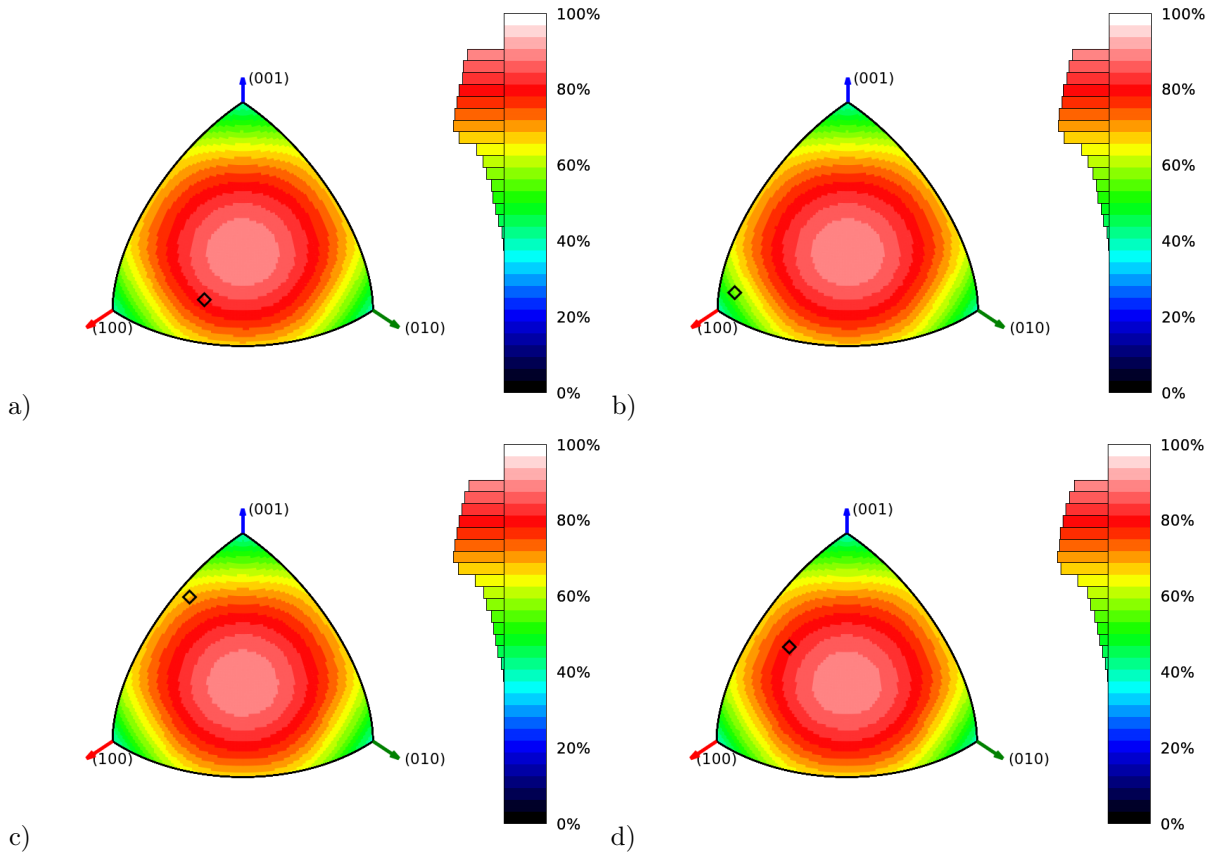

Figure S2.11: Potency maps for chosen pressure point for synchrotron series:
a) 0002_1p62GPa, potency: 0.8110 (min: 0.3928, max: 0.9055, average: 0.7286),
b) 0003_1p62GPa, potency: 0.5665 (min: 0.3932, max: 0.9058, average: 0.7290),
c) 0004_1p62GPa, potency: 0.6859 (min: 0.3904, max: 0.9043, average: 0.7271),
d) 0005_1p62GPa, potency: 0.7971 (min: 0.3890, max: 0.9029, average: 0.7259).
Directions on graphs are consistent with $Pca2_1$ space group instead of $Pb2_1a$ space group.
Average potency from all crystals: 0.7151 – similar to theoretical average potency calculated by DTool.

S2.2 Hydrostatic limits for different PTMs

Silicone oils are reported as having a hydrostatic limit from 0.9 GPa to 3.0 GPa [Klotz *et al.*(2009)Klotz, Chervin, Munsch, and Le Ma Angel *et al.*(2007)Angel, Bujak, Zhao, Gatta, and Jacobsen] depending on the exact variant. Pressure dependencies of the unit cell parameters show that our particular oil may act as non-hydrostatic above 2.0 GPa. This hypothesis could be further supported by the fact, that maximum pressure at which structure of **ArPEt** could be solved and refined when applying this PTM is 2.13 GPa. The n-pentane and i-pentane 1:1 mixture is reported quasi-hydrostatic up to 7.4 GPa and Daphne-7575 has hydrostatic limit of 6.5 GPa [Klotz *et al.*(2009)Klotz, Chervin, Munsch, and Le Marchand], so they are expected to provide isotropic compression of **ArPEt** in the studied pressure range (up to 3.30 GPa).

S2.3 Pressures

Table S2.1: Pressure points for *in-house* diffraction experiments series. Nominal uncertainties of pressure determination were in range 0.03–0.04 GPa. Points marked by asterisk (*) relate to pressures at which diffraction experiments have been done but structure was not determined (crystal broke into to many pieces). Structure from pressure point marked by (**) was non-solvable.

Non-hydrostatic medium (silicone oil)

Series	Pressure [GPa]										
1 (appr2)	0.26	–	–	0.57	0.89	1.12	1.43	1.89	–	2.42*	–
2 (appr4)	0.16	0.32	0.45	0.72*	–	–	–	–	–	–	–
3 (appr5)	–	0.33	–	0.64	–	–	–	–	2.13	2.42*	–

Quasi-hydrostatic medium (n-pentane/i-pentane 1:1 mixture)

Series	Pressure [GPa]										
4 (appr6)	–	–	–	0.58	0.94	–	1.64	1.94	2.16**	2.31	2.59

Table S2.2: Pressure points for synchrotron diffraction experiments series. Nominal uncertainties of pressure determination were in range 0.03–0.04 GPa.

Quasi-hydrostatic medium (Daphne-7575)

Series	Pressure [GPa]				
synchrotron	1.62	1.80	2.16	2.66	3.30

S2.4 Data processing, structure solution and refinement

Hydrogen atoms were placed based on carbon atoms geometry. Atomic displacement parameters for hydrogen atoms were refined isotropically and for remaining atoms – anisotropically. Structure from atmospheric pressure was refined without additional restrains. For structures from high-pressure data there was no need to add restrains to molecules geometry expect same bond distances in disordered structures. Remain used restrains relate to atomic displacement parameters modeling to avoid non-physical values.

Table S2.3: Unit cell metrics, selected crystallographic data and refinement statistics for *in-house* experiments – part 1.

Empirical formula	$C_{15}H_{22}AuOP$				
Formula weight $[\frac{g}{mol}]$	446.26				
Identification code	appr0_1atm	appr2_0p26GPa	appr2_0p57GPa	appr2_0p89GPa	appr2_1p12GPa
Temperature [K]	293(2)	295.3(10)	295.8(2)	295.65(16)	295.5(5)
Pressure [GPa]	0.0001	0.26	0.57	0.89	1.12
Opening angle [°]	–	52	52	52	52
Crystal system	orthorhombic	orthorhombic	orthorhombic	orthorhombic	orthorhombic
Space group	$Pbca$	$Pbca$	$Pb2_1a$	$Pb2_1a$	$Pb2_1a$
a [Å]	16.3373(7)	16.1780(6)	17.1700(18)	17.3429(4)	17.1407(10)
b [Å]	11.3081(5)	11.1922(3)	9.9744(5)	9.9201(2)	9.8864(4)
c [Å]	17.9484(8)	17.8018(8)	17.6072(15)	16.9287(5)	16.8388(12)
α, β, γ [°]	90, 90, 90	90, 90, 90	90, 90, 90	90, 90, 90	90, 90, 90
Volume [Å^3]	3315.9(3)	3223.3(2)	3015.4(4)	2912.47(12)	2853.5(3)
Z	8	8	8	8	8
ρ_{calc} $[\frac{g}{cm^3}]$	1.788	1.839	1.966	2.035	2.078
μ $[mm^{-1}]$	4.843	4.982	5.325	5.513	5.627
F(000)	1712	1712	1712	1712	1712
Crystal size $[mm^3]$	0.59 x 0.28 x 0.17	0.18 x 0.13 x 0.09	0.18 x 0.13 x 0.09	0.18 x 0.13 x 0.09	0.18 x 0.13 x 0.09
Radiation source	Ag Kα	Ag Kα	Ag Kα	Ag Kα	Ag Kα
Radiation wavelength [Å]	0.56087	0.56087	0.56087	0.56087	0.56087
2θ range	3.894 to 52.746	3.932 to 42.142	3.744 to 43.786	3.706 to 54.058	3.75 to 46.004
Reflections collected	14048	41474	31068	52871	40946
R_{int}	0.0341	0.0791	0.1107	0.0618	0.0873
Resolution [Å]	0.6313	0.7800	0.7521	0.6171	0.7177
Completeness	0.984	0.929	0.906	0.912	0.914
Data; restraints; parameters	6050; 0; 239	3269; 224; 251	6258; 1; 334	10223; 1; 334	7156; 1; 334
R_1, wR_2 ($I > 2\sigma(I)$)	0.0464, 0.0761	0.0328, 0.0452	0.0476, 0.0779	0.0382, 0.0475	0.0440, 0.0864
R_1, wR_2 (all data)	0.1300, 0.1036	0.0915, 0.0572	0.0821, 0.0910	0.0882, 0.0564	0.0691, 0.0982
Largest diff. peak/hole [eÅ^{-3}]	0.794/-0.589	0.563/-0.476	1.516/-1.701	1.194/-1.026	1.981/-1.439
Flack parameter	–	–	0.52(4)	0.457(18)	0.54(3)

Table S2.4: Unit cell metrics, selected crystallographic data and refinement statistics for *in-house* experiments – part 2.

Empirical formula	$C_{15}H_{22}AuOP$				
Formula weight $[\frac{g}{mol}]$	446.26				
Identification code	appr22_1p43GPa	appr2_1p89GPa	appr4_0p16GPa	appr4_0p32GPa	appr4_0p45GPa
Temperature [K]	295.6(3)	295.2(6)	295.1(4)	295.40(16)	295.3(4)
Pressure [GPa]	1.43	1.89	0.16	0.32	0.45
Opening angle [°]	52	52	38	38	38
Crystal system	orthorhombic	orthorhombic	orthorhombic	orthorhombic	orthorhombic
Space group	$Pb2_1a$	$Pb2_1a$	$Pbca$	$Pbca$	$Pbca$
a [Å]	17.0578(5)	16.9596(8)	16.527(3)	16.215(3)	16.168(2)
b [Å]	9.8693(2)	9.8810(3)	11.2886(14)	11.0942(12)	10.9575(12)
c [Å]	16.7532(6)	16.6423(12)	17.901(13)	17.732(4)	17.526(4)
α, β, γ [°]	90, 90, 90	90, 90, 90	90, 90, 90	90, 90, 90	90, 90, 90
Volume [Å^3]	2820.38(14)	2788.9(3)	3340(2)	3189.9(10)	3104.8(10)
Z	8	8	8	8	8
ρ_{calc} $[\frac{g}{cm^3}]$	2.102	2.126	1.775	1.858	1.909
μ $[mm^{-1}]$	5.693	5.758	4.808	5.034	5.172
F(000)	1712	1712	1712	1712	1712
Crystal size $[mm^3]$	0.18 x 0.13 x 0.09	0.18 x 0.13 x 0.09	0.14 x 0.09 x 0.06	0.14 x 0.09 x 0.06	0.14 x 0.09 x 0.06
Radiation source	Ag Kα	Ag Kα	Ag Kα	Ag Kα	Ag Kα
Radiation wavelength [Å]	0.56087	0.56087	0.56087	0.56087	0.56087
2θ range	3.768 to 54.022	3.79 to 53.842	3.888 to 41.036	3.95 to 41.028	3.976 to 50.99
Reflections collected	49031	49554	7576	8296	10035
R_{int}	0.0596	0.0742	0.0885	0.0837	0.0783
Resolution [Å]	0.6175	0.6194	0.8001	0.8002	0.6515
Completeness	0.914	0.914	0.484	0.703	0.723
Data; restraints; parameters	9888; 1; 334	9749; 1; 334	1596; 252; 225	2239; 228; 227	3319; 206; 227
R_1, wR_2 ($I > 2\sigma(I)$)	0.0381, 0.0488	0.0450, 0.0571	0.0440, 0.0712	0.0525, 0.0657	0.0537, 0.0892
R_1, wR_2 (all data)	0.0816, 0.0571	0.1038, 0.0682	0.1751, 0.1075	0.1764, 0.0953	0.2449, 0.1402
Largest diff. peak/hole [eÅ^{-3}]	1.065/ -0.966	1.092/-1.621	0.424/-0.303	0.623/-0.409	0.637/-0.843
Flack parameter	0.483(17)	0.58(2)	–	–	–

Table S2.5: Unit cell metrics, selected crystallographic data and refinement statistics for *in-house* experiments – part 3.

Empirical formula	$C_{15}H_{22}AuOP$				
Formula weight $[\frac{g}{mol}]$	446.26				
Identification code	appr5_0p33GPa	appr5_0p64GPa	appr5_2p13GPa	appr6_0p58GPa	appr6_0p94GPa
Temperature [K]	295.5(3)	294.3(6)	294.7(3)	293(2)	293(2)
Pressure [GPa]	0.33	0.64	2.13	0.58	0.94
Opening angle [°]	51	51	51	39	39
Crystal system	orthorhombic	orthorhombic	monoclinic	orthorhombic	orthorhombic
Space group	$Pbca$	$Pb2_1a$	$P11a$	$Pb2_1a$	$Pb2_1a$
a [Å]	16.0628(9)	17.6564(8)	16.7021(6)	17.5579(5)	17.2929(5)
b [Å]	11.0945(4)	9.9742(4)	9.8830(3)	9.9652(4)	9.9154(4)
c [Å]	17.7070(6)	17.1118(5)	16.8029(4)	17.0487(9)	16.8744(7)
α, β, γ [°]	90, 90, 90	90, 90, 90	90, 90, 93.865(3)	90, 90, 90	90, 90, 90
Volume [Å^3]	3155.5(2)	3013.5(2)	2767.29(14)	2983.0(2)	2893.39(17)
Z	8	8	8	8	8
ρ_{calc} $[\frac{g}{cm^3}]$	1.879	1.967	2.142	1.987	2.049
μ $[mm^{-1}]$	5.089	5.328	5.803	5.383	5.550
F(000)	1712	1712	1712	1712	1712
Crystal size $[mm^3]$	0.14 x 0.12 x 0.11	0.14 x 0.12 x 0.11	0.14 x 0.12 x 0.11	0.16 x 0.12 x 0.10	0.16 x 0.12 x 0.10
Radiation source	Ag Kα	Ag Kα	Ag Kα	AgKα	Ag Kα
Radiation wavelength [Å]	0.56087	0.56087	0.56087	0.56087	0.56087
2θ range	3.63 to 41.02	3.64 to 51.446	5.026 to 41.954	3.662 to 42.71	4.932 to 42.202
Reflections collected	35162	45778	22719	17619	12415
R_{int}	0.0850	0.0906	0.0547	0.0506	0.0479
Resolution [Å]	0.8004	0.6461	0.7834	0.7701	0.7790
Completeness	0.919	0.928	0.651	0.722	0.741
Data; restraints; parameters	2939; 204; 238	9388; 1; 334	7038; 410; 666	4264; 67; 334	3426; 115; 334
R_1, wR_2 ($I > 2\sigma(I)$)	0.0522, 0.1311	0.0472, 0.0505	0.0432, 0.0630	0.0359, 0.0508	0.0395, 0.0447
R_1, wR_2 (all data)	0.1092, 0.1734	0.1365, 0.0640	0.0749, 0.0711	0.0871, 0.0640	0.0830, 0.0524
Largest diff. peak/hole [eÅ^{-3}]	1.075/-1.755	0.881/-0.700	0.926/-0.971	1.099/-1.174	0.871/-0.676
Flack parameter	–	0.07(2)	0.06(3)	0.71(3)	0.69(4)

Table S2.6: Unit cell metrics, selected crystallographic data and refinement statistics for *in-house* experiments – part 4.

Empirical formula	$C_{15}H_{22}AuOP$			
Formula weight $[\frac{g}{mol}]$	446.26			
Identification code	appr6_1p64GPa	appr6_1p94GPa	appr6_2p31GPa	appr6_2p59GPa
Temperature [K]	293(2)	293(2)	293(2)	293(2)
Pressure [GPa]	1.64	1.94	2.31	2.59
Opening angle [°]	38.5	38.5	38	37
Crystal system	orthorhombic	orthorhombic	orthorhombic	orthorhombic
Space group	$Pb2_1a$	$Pb2_1a$	$Pbca$	$Pbca$
a [Å]	17.0308(6)	16.9003(5)	16.9137(6)	16.7686(6)
b [Å]	9.8580(5)	9.8370(4)	9.8518(5)	9.8173(2)
c [Å]	16.7203(11)	16.6364(10)	16.3267(11)	16.1828(17)
α, β, γ [°]	90, 90, 90	90, 90, 90	90, 90, 90	90, 90, 90
Volume [Å^3]	2807.2(3)	2765.8(2)	2720.5(2)	2664.1(3)
Z	8	8	8	8
ρ_{calc} $[\frac{g}{cm^3}]$	2.112	2.143	2.179	2.225
μ $[mm^{-1}]$	5.720	5.806	5.902	6.027
F(000)	1712	1712	1712	1712
Crystal size $[mm^3]$	0.16 x 0.12 x 0.10	0.16 x 0.12 x 0.10	0.16 x 0.12 x 0.10	0.16 x 0.12 x 0.10
Radiation source	Ag Kα	Ag Kα	Ag Kα	Ag Kα
Radiation wavelength [Å]	0.56087	0.56087	0.56087	0.56087
2θ range	3.774 to 51.308	3.804 to 51.218	3.8 to 51.244	3.834 to 51.376
Reflections collected	17793	17169	13822	11137
R_{int}	0.0630	0.0652	0.0767	0.1009
Resolution [Å]	0.6478	0.6488	0.6485	0.6470
Completeness	0.737	0.724	0.700	0.639
Data; restraints; parameters	5367; 151; 334	5195; 229; 334	2984; 6; 166	2732; 6; 167
R_1, wR_2 ($I > 2\sigma(I)$)	0.0536, 0.0988	0.0477, 0.0524	0.0830, 0.1640	0.0464, 0.0601
R_1, wR_2 (all data)	0.1401, 0.1343	0.1070, 0.0626	0.1346, 0.1808	0.1155, 0.0747
Largest diff. peak/hole [eÅ^{-3}]	1.871/-2.894	1.242/-0.843	3.094/-2.572	1.166/-1.014
Flack parameter	0.35(5)	0.70(3)	–	–

Table S2.7: Unit cell metrics, selected crystallographic data and refinement statistics for synchrotron experiments – part 1.

Empirical formula	$C_{15}H_{22}AuOP$			
Formula weight $[\frac{g}{mol}]$	446.26			
Temperature [K]	293(2)			
Pressure [GPa]	1.62			
Opening angle [°]	39			
Identification code	0002_1p62GPa	0003_1p62GPa	0004_1p62GPa	0005_1p62GPa
Crystal system	orthorhombic	orthorhombic	orthorhombic	orthorhombic
Space group	$Pb2_1a$	$Pb2_1a$	$Pb2_1a$	$Pb2_1a$
a [Å]	17.0210(5)	17.0148(15)	17.0137(3)	17.0066(3)
b [Å]	9.85683(19)	9.85340(19)	9.85586(8)	9.85656(13)
c [Å]	16.7157(3)	16.7117(3)	16.7032(5)	16.7104(3)
α, β, γ [°]	90, 90, 90	90, 90, 90	90, 90, 90	90, 90, 90
Volume [$Å^3$]	2804.45(12)	2801.8(3)	2800.87(9)	2801.12(7)
Z	8	8	8	8
ρ_{calc} $[\frac{g}{cm^3}]$	2.114	2.116	2.117	2.116
μ $[mm^{-1}]$	2.577	2.579	2.580	2.580
F(000)	1712	1712	1712	1712
Crystal size $[mm^3]$	0.002 x 0.0015 x 0.001	0.002 x 0.002 x 0.001	0.0025 x 0.002 x 0.0015	0.004 x 0.0015 x 0.001
Radiation source	synchrotron	synchrotron	synchrotron	synchrotron
Radiation wavelength [Å]	0.410	0.410	0.410	0.410
2θ range	3.092 to 43.174	3.91 to 43.078	3.094 to 43.434	3.1 to 43.632
Reflections collected	10170	9214	10054	10372
R_{int}	0.0308	0.0326	0.0334	0.0254
Resolution [Å]	0.5572	0.5584	0.5540	0.5516
Completeness	0.808	0.606	0.632	0.811
Data; restraints; parameters	7714; 1; 334	5712; 1; 334	6267; 1; 334	7208; 1; 334
R_1, wR_2 ($I > 2\sigma(I)$)	0.0412, 0.1017	0.0335, 0.0757	0.0299, 0.0802	0.0326, 0.0832
R_1, wR_2 (all data)	0.0584, 0.1116	0.0557, 0.0845	0.0325, 0.0819	0.0365, 0.0863
Largest diff. peak/hole [e$Å^{-3}$]	1.722/ -1.151	0.925/-1.166	1.210/-0.618	2.221/ -0.690
Flack parameter	0.30(4)	0.71(5)	0.94(3)	0.30(3)

Table S2.8: Unit cell metrics, selected crystallographic data and refinement statistics for synchrotron experiments – part 2.

Empirical formula	$C_{15}H_{22}AuOP$			
Formula weight $[\frac{g}{mol}]$	446.26			
Temperature [K]	293(2)			
Pressure [GPa]	1.80			
Opening angle [°]	39			
Identification code	0006_1p80GPa	0007_1p80GPa	0008_1p80GPa	0009_1p80GPa
Crystal system	orthorhombic	orthorhombic	orthorhombic	orthorhombic
Space group	$Pb2_1a$	$Pb2_1a$	$Pb2_1a$	$Pb2_1a$
a [Å]	16.9414(8)	16.9382(13)	16.9319(3)	16.9299(3)
b [Å]	9.8439(2)	9.83503(15)	9.83974(8)	9.84107(14)
c [Å]	16.6593(5)	16.6637(2)	16.6583(5)	16.6630(3)
α, β, γ [°]	90, 90, 90	90, 90, 90	90, 90, 90	90, 90, 90
Volume [$Å^3$]	2778.27(17)	2776.0(2)	2775.36(9)	2776.20(8)
Z	8	8	8	8
ρ_{calc} $[\frac{g}{cm^3}]$	2.134	2.136	2.136	2.135
μ $[mm^{-1}]$	2.601	2.603	2.604	2.603
F(000)	1712	1712	1712	1712
Crystal size $[mm^3]$	0.002 x 0.0015 x 0.001	0.002 x 0.002 x 0.001	0.0025 x 0.002 x 0.0015	0.004 x 0.0015 x 0.001
Radiation source	synchrotron	synchrotron	synchrotron	synchrotron
Radiation wavelength [Å]	0.410	0.410	0.410	0.410
2θ range	3.1 to 43.338	3.924 to 43.602	3.1 to 43.296	3.114 to 43.1
Reflections collected	9295	9876	9975	10302
R_{int}	0.0646	0.0351	0.0347	0.0249
Resolution [Å]	0.5552	0.5520	0.5557	0.5581
Completeness	0.757	0.609	0.631	0.808
Data; restraints; parameters	7228; 1; 334	5867; 1; 334	6181; 1; 334	7103; 1; 334
R_1, wR_2 ($I > 2\sigma(I)$)	0.0728, 0.1895	0.0368, 0.0873	0.0301, 0.0802	0.0322, 0.0811
R_1, wR_2 (all data)	0.1044, 0.2095	0.0500, 0.0928	0.0329, 0.0821	0.0366, 0.0840
Largest diff. peak/hole [e$Å^{-3}$]	2.618/-2.175	1.104/-0.599	1.370/-0.671	2.346/ -0.671
Flack parameter	0.68(7)	0.63(4)	0.10(3)	0.59(3)

Table S2.9: Unit cell metrics, selected crystallographic data and refinement statistics for synchrotron experiments – part 3.

Empirical formula	$C_{15}H_{22}AuOP$			
Formula weight $[\frac{g}{mol}]$	446.26			
Temperature [K]	293(2)			
Pressure [GPa]	2.16			
Opening angle [°]	39			
Identification code	0010_2p16GPa	0011_2p16GPa	0012_2p16GPa	0013_2p16GPa
Crystal system	orthorhombic	orthorhombic	orthorhombic	orthorhombic
Space group	$Pbca$	$Pb2_1a$	$Pbca$	$Pbca$
a [Å]	16.8614(15)	16.7860(17)	16.8809(4)	16.8830(3)
b [Å]	9.8359(4)	9.80510(19)	9.84471(12)	9.85238(17)
c [Å]	16.3043(9)	16.5696(3)	16.2781(8)	16.2916(4)
α, β, γ [°]	90, 90, 90	90, 90, 90	90, 90, 90	90, 90, 90
Volume [Å^3]	2704.0(3)	2727.2(3)	2705.21(14)	2709.90(9)
Z	8	8	8	8
ρ_{calc} $[\frac{g}{cm^3}]$	2.192	2.174	2.191	2.188
μ $[mm^{-1}]$	2.672	2.650	2.671	2.666
F(000)	1712	1712	1712	1712
Crystal size $[mm^3]$	0.002 x 0.0015 x 0.001	0.002 x 0.002 x 0.001	0.0025 x 0.002 x 0.0015	0.004 x 0.0015 x 0.001
Radiation source	synchrotron	synchrotron	synchrotron	synchrotron
Radiation wavelength [Å]	0.410	0.410	0.410	0.410
2θ range	3.118 to 43.406	3.948 to 43.334	3.116 to 43.384	3.202 to 43.576
Reflections collected	9095	9573	9689	9605
R_{int}	0.1302	0.0410	0.0318	0.0373
Resolution [Å]	0.5544	0.5552	0.5546	0.5523
Completeness	0.823	0.612	0.656	0.817
Data; restraints; parameters	4454; 0; 167	5763; 49; 334	3652; 0; 167	4272; 0; 167
R_1, wR_2 ($I > 2\sigma(I)$)	0.1214, 0.3105	0.0488, 0.1240	0.0309, 0.0870	0.0419, 0.1153
R_1, wR_2 (all data)	0.1884, 0.3593	0.0721, 0.1351	0.0367, 0.0900	0.0520, 0.1217
Largest diff. peak/hole [eÅ^{-3}]	3.142/-3.500	1.672/-1.079	1.501/-0.640	1.617/-2.294
Flack parameter	–	0.58(6)	–	–

Table S2.10: Unit cell metrics, selected crystallographic data and refinement statistics for synchrotron experiments – part 4.

Empirical formula	$C_{15}H_{22}AuOP$			
Formula weight $[\frac{g}{mol}]$	446.26			
Temperature [K]	293(2)			
Pressure [GPa]	2.66			
Opening angle [°]	39		38	
Identification code	0013a_2p66GPa	0014_2p66GPa	0015_2p66GPa	0016_2p66GPa
Crystal system	orthorhombic	orthorhombic	orthorhombic	orthorhombic
Space group	$Pbca$	$Pbca$	$Pbca$	$Pbca$
a [Å]	16.7535(5)	16.758(2)	16.7442(3)	16.7395(3)
b [Å]	9.80417(16)	9.8015(2)	9.80349(10)	9.79915(17)
c [Å]	16.1656(3)	16.1729(3)	16.1545(6)	16.1723(3)
α, β, γ [°]	90, 90, 90	90, 90, 90	90, 90, 90	90, 90, 90
Volume [Å^3]	2655.27(10)	2656.5(4)	2651.79(11)	2652.79(9)
Z	8	8	8	8
ρ_{calc} $[\frac{g}{cm^3}]$	2.233	2.232	2.236	2.235
μ $[mm^{-1}]$	2.721	2.720	2.725	2.724
F(000)	1712	1712	1712	1712
Crystal size $[mm^3]$	0.002 x 0.0015 x 0.001	0.002 x 0.002 x 0.001	0.0025 x 0.002 x 0.0015	0.004 x 0.0015 x 0.001
Radiation source	synchrotron	synchrotron	synchrotron	synchrotron
Radiation wavelength [Å]	0.410	0.410	0.410	0.410
2θ range	3.134 to 43.17	3.226 to 42.982	3.134 to 43.468	3.226 to 43.276
Reflections collected	9397	8143	9105	9292
R_{int}	0.0385	0.0635	0.0474	0.0445
Resolution [Å]	0.5572	0.5596	0.5536	0.5559
Completeness	0.829	0.602	0.608	0.806
Data; restraints; parameters	4402; 0; 167	3213; 66; 167	3181; 0; 167	4033; 0; 167
R_1, wR_2 ($I > 2\sigma(I)$)	0.0313, 0.0825	0.0718, 0.1814	0.0466, 0.1193	0.0420, 0.1340
R_1, wR_2 (all data)	0.0450, 0.0896	0.0923, 0.1944	0.0540, 0.1256	0.0495, 0.1417
Largest diff. peak/hole [eÅ^{-3}]	1.196/-1.288	3.949/-3.077	2.831/-2.362	2.859/-2.323
Flack parameter	–	–	–	–

Table S2.11: Unit cell metrics, selected crystallographic data and refinement statistics for synchrotron experiments – part 5.

Empirical formula	$C_{15}H_{22}AuOP$		
Formula weight [$\frac{g}{mol}$]	446.26		
Temperature [K]	293(2)		
Pressure [GPa]	3.30		
Opening angle [°]	38		39
Identification code	0017_3p30GPa	0019_3p30GPa	0021_3p30GPa
Crystal system	orthorhombic	orthorhombic	orthorhombic
Space group	$Pbca$	$Pbca$	$Pbca$
a [Å]	16.5856(7)	16.5789(3)	16.5751(3)
b [Å]	9.7494(2)	9.75229(9)	9.7432(2)
c [Å]	16.0285(4)	16.0089(5)	16.0297(3)
α, β, γ [°]	90, 90, 90	90, 90, 90	90, 90, 90
Volume [Å^3]	2591.80(13)	2588.35(10)	2588.71(9)
Z	8	8	8
ρ_{calc} [$\frac{g}{cm^3}$]	2.287	2.290	2.290
μ [mm^{-1}]	2.788	2.792	2.791
F(000)	1712	1712	1712
Crystal size [mm^3]	0.002 x 0.0015 x 0.001	0.0025 x 0.002 x 0.0015	0.004 x 0.0015 x 0.001
Radiation source	synchrotron	synchrotron	synchrotron
Radiation wavelength [Å]	0.410	0.410	0.410
2θ range	3.998 to 43.15	3.156 to 43.398	3.256 to 43.53
Reflections collected	8880	8771	9352
R_{int}	0.0479	0.0321	0.0272
Resolution [Å]	0.5575	0.5545	0.5529
Completeness	0.811	0.622	0.825
Data; restraints; parameters	4215; 0; 167	3220; 0; 167	4079; 0; 167
R_1, wR_2 ($I > 2\sigma(I)$)	0.0363, 0.0784	0.0234, 0.0627	0.0321, 0.0946
R_1, wR_2 (all data)	0.0638, 0.0862	0.0264, 0.0645	0.0397, 0.1010
Largest diff. peak/hole [eÅ^{-3}]	1.177/-1.120	0.731/-0.860	2.768/-2.263
Flack parameter	–	–	–

S2.5 Merging results

Merging datasets from high-pressure experiments enable achieving better reciprocal space coverage and data completeness. It is important to merge datasets from the same conditions. In this purpose, four crystal specimens were placed in one DAC (Figure S2.12). Merging results are shown in Table S2.12. At 2.16 GPa two different merging processes were proceeded. First – for crystals B and C – in P$b2_1a$ space group. It was original space group (based on systematic extinctions) only for crystal B. Structure of crystal C was solved in lower-symmetry space group (P$b2_1a$ instead of Pbca) to maintain same asymmetric unit and symmetry with data from crystal B. Second – for crystals C and D – in Pbca space group, which was original space group for both crystals. This first merging resulted in high-complete data, but with worse R_{merge} and non-solvable structure.

Figure S2.12: Crystal specimens in DAC for synchrotron measurements.

Table S2.12: Merging results for synchrotron datasets.

Pressure [GPa]	Input			Output		
(Space group)	File	R_{int}	Completeness	File	R_{merge}	Completeness
1.62	0002 (**A**)	3.08%	80.8%	p1m1	4.25%	95.3%
(P$b2_1a$)	0003 (**B**)	3.26%	60.6%			
	0004 (**C**)	3.34%	63.2%			
	0005 (**D**)	2.54%	81.1%			
1.80	0006 (**A**)	6.46%	75.7%	p2m1	5.13%	95.2%
(P$b2_1a$)	0007 (**B**)	3.51%	60.9%			
	0008 (**C**)	3.47%	63.1%			
	0009 (**D**)	2.49%	80.8%			
2.16	0011 (**B**)	4.10%	61.2%	p3m1	16.01%	90.0%
(P$b2_1a$)	0012 (**C**)	2.91%	65.6%			
2.16	0012 (**C**)	3.18%	65.6%	p3m2	5.62%	87.6%
(Pbca)	0013 (**D**)	3.73%	81.7%			
2.66	0013a (**A**)	3.85%	82.9%	p4m1	5.85%	95.5%
(Pbca)	0014 (**B**)	6.35%	60.2%			
	0015 (**C**)	4.74%	60.8%			
	0016 (**D**)	4.45%	80.6%			
3.30	0017 (**A**)	4.79%	81.1%	p5m1	5.40%	93.0%
(Pbca)	0019 (**C**)	3.21%	62.2%			
	0021 (**D**)	2.72%	82.5%			

Table S2.13: Unit cell metrics, selected crystallographic data and refinement statistics for merged datasets.

Empirical formula	$C_{15}H_{22}AuOP$				
Formula weight $[\frac{g}{mol}]$	446.26				
Temperature [K]	293(2)				
Identification code	p1m1_1p62GPa	p2m1_1p80GPa	p3m2_2p16GPa	p4m1_2p66GPa	p5m1_3p30GPa
Pressure [GPa]	1.62	1.8	2.16	2.66	3.3
Opening angle [°]	39	39	39	38	38
Crystal system	orthorhombic	orthorhombic	orthorhombic	orthorhombic	orthorhombic
Space group	$Pb2_1a$	$Pb2_1a$	$Pbca$	$Pbca$	$Pbca$
a [Å]	17.0140(4)	16.9414(8)	16.8830(3)	16.7395(3)	16.5856(7)
b [Å]	9.85573(8)	9.8439(2)	9.85238(17)	9.79915(17)	9.7494(2)
c [Å]	16.71022(18)	16.6593(5)	16.2916(4)	16.1723(3)	16.0285(4)
α, β, γ [°]	90, 90, 90	90, 90, 90	90, 90, 90	90, 90, 90	90, 90, 90
Volume [Å^3]	2802.06(7)	2778.27(17)	2709.90(9)	2652.79(9)	2591.80(13)
Z	8	8	8	8	8
Radiation source	synchrotron	synchrotron	synchrotron	synchrotron	synchrotron
Radiation wavelength [Å]	0.410	0.410	0.410	0.410	0.410
2θ range	3.092 to 43.63	3.1 to 43.386	3.114 to 43.576	3.134 to 43.466	3.158 to 43.53
Reflections collected	27326	26965	20069	37626	28104
R_{int}	0.0407	0.0524	0.0562	0.0584	0.0540
Resolution [Å]	0.5517	0.5546	0.5523	0.5536	0.5529
Completeness	0.953	0.952	0.876	0.955	0.930
Data; restraints; parameters	11909; 1; 334	11834; 1; 334	4974; 0; 167	5873; 0; 167	5415; 0; 167
R_1, wR_2 ($I > 2\sigma(I)$)	0.0307, 0.0722	0.0357, 0.0769	0.0508, 0.1241	0.0509, 0.1082	0.0406, 0.0955
R_1, wR_2 (all data)	0.0429, 0.0756	0.0482, 0.0842	0.0597, 0.1308	0.0606, 0.1135	0.0566, 0.1039
Largest diff. peak/hole [eÅ^{-3}]	1.996/-1.373	2.360/-1.345	2.589/-2.063	1.620/-2.557	3.071/-1.499
Flack parameter	0.56(2)	0.46(3)	–	–	–

S2.6 CCDC deposition numbers

Table S2.14: text

Identification code	CCDC number
appr0_1atm	2370910
appr2_0p26GPa	2370856
appr2_0p57GPa	2370854
appr2_0p89GPa	2370859
appr2_1p12GPa	2370855
appr2_1p43GPa	2370857
appr2_1p89GPa	2370858
appr4_0p16GPa	2370873
appr4_0p32GPa	2370878
appr4_0p45GPa	2370874
appr5_0p33GPa	2370876
appr5_0p64GPa	2370877
appr5_2p13GPa	2370875
appr6_0p58GPa	2370887
appr6_0p94GPa	2370883
appr6_1p64GPa	2370885
appr6_1p94GPa	2370886
appr6_2p31GPa	2370884
appr6_2p59GPa	2370882

Identification code	CCDC number
0002_1p62GPa	2370902
0003_1p62GPa	2370904
0004_1p62GPa	2370903
0005_1p62GPa	2370909
0006_1p80GPa	2370908
0007_1p80GPa	2370906
0008_1p80GPa	2370907
0009_1p80GPa	2370905
0010_2p16GPa	2370917
0011_2p16GPa	2370919
0012_2p16GPa	2370916
0013_2p16GPa	2370920
0013a_2p66GPa	2370914
0014_2p66GPa	2370921
0015_2p66GPa	2370915
0016_2p66GPa	2370918
0017_3p30GPa	2370937
0019_3p30GPa	2370938
0021_3p30GPa	2370936

Identification code	CCDC number
p1m1_1p62GPa	2370943
p2m1_1p80GPa	2370939
p3m2_2p16GPa	2370941
p4m1_2p66GPa	2370942
p5m1_3p30GPa	2370940

S3 Photoluminescence and its variability at increased pressure

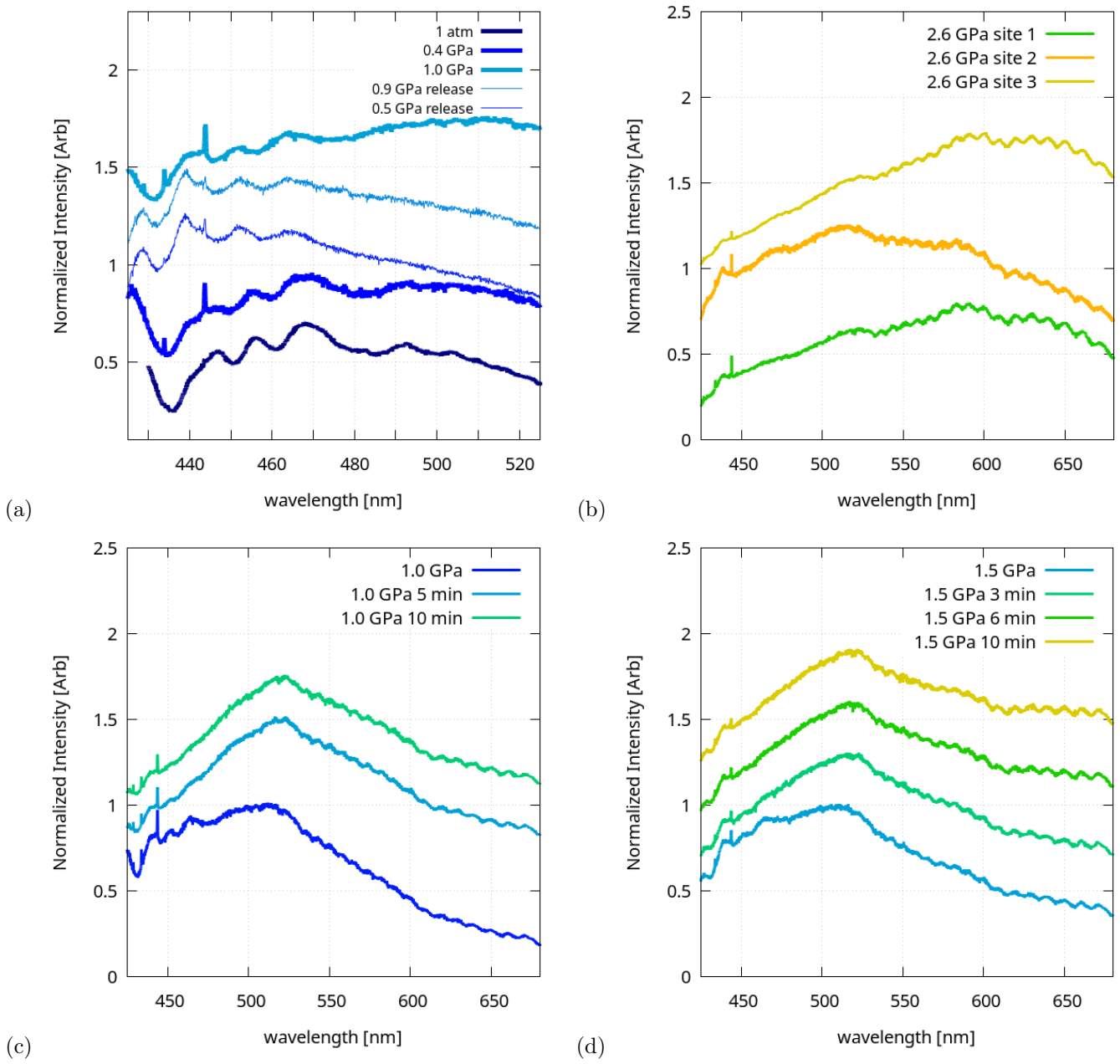

Figure S3.13: Fluorescence spectra of single crystal of **ArPEt** placed inside a DAC in n-pentane:i-pentane mixture and their variability (a) with pressure in low-pressure range; (b) with three different sites on the single-crystal face at 2.6 GPa; (c,d) at several time-delays after pressure increase to 1.0 GPa and 1.5 GPa accordingly. Presence of the phase **ArPEt-III** at 2.6 GPa has been confirmed by SCXRD experiment. The colors chosen arbitrarily to differentiate between the spectra. Persistent spike at 444 nm represents the Raman peak of the diamonds in a DAC. All spectra were normalized to their maximum value and plotted with increments along the vertical axis for clarity.

S4 Phase transitions

S4.1 Disorder below 0.5 GPa

ArPEt-I phase was obtained in pressure range from atmospheric up to about 0.5 GPa. All structures are disordered with percentage of second conformer showed in Table S4.15. For series 1 and 3 contribution was initially lower than for 2. Importantly, screening and pre-experiment for crystal of 2 series was performed at 100K instead of 300K. Impact of temperature on second conformer contribution will be studied in detail in future. For now, results suggest that mainly conformer with **C** triethylphosphine conformation takes part in first phase transition.

Table S4.15: Contribution of second conformer (with **F** triethylphosphine conformation) in **ArPEt-I** phase by measurement series.

Series	1 (appr2)	3 (appr5)	2 (appr4)		
Pressure [GPa]	0.26	0.33	0.16	0.32	0.45
Second conformer contribution [%]	29	25	42	35	27

S4.2 Reciprocal layers

Phase transitions were confirmed by systematic extinctions on reciprocal layers. Some of them (near phase transition points) are shown below (Figure S4.14 – S4.16).

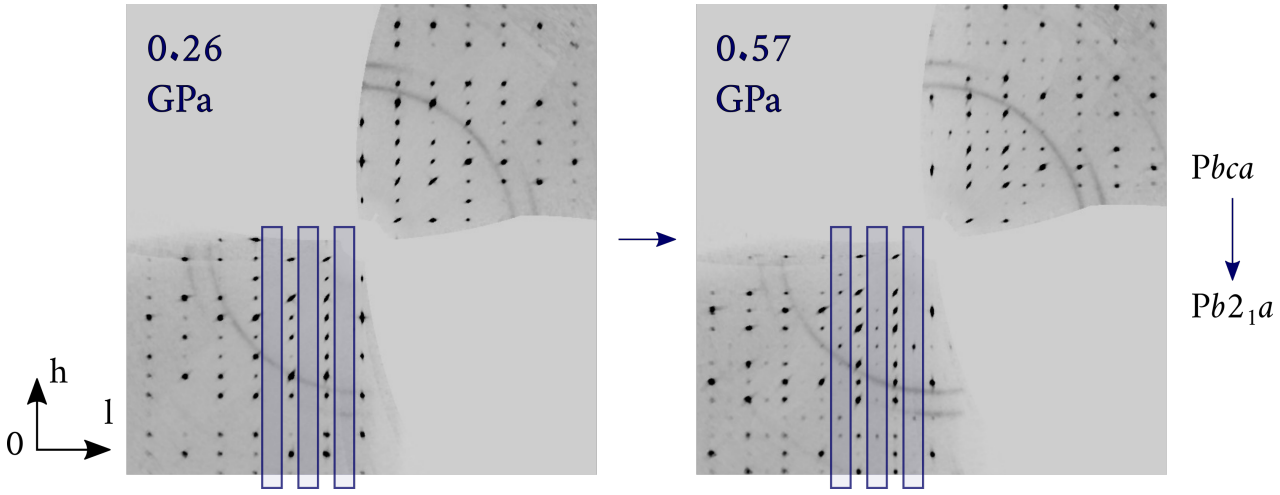

Figure S4.14: First phase transition analysis on layer *h0l* for series 1. Region where reflection from $\mathbf{c}_{[010]}$ glide plane should be extinct ($l = 2n + 1$) is framed. Reflections in this region at 0.57 GPa confirms phase transformation P$bca \rightarrow$ P$b2_1a$.

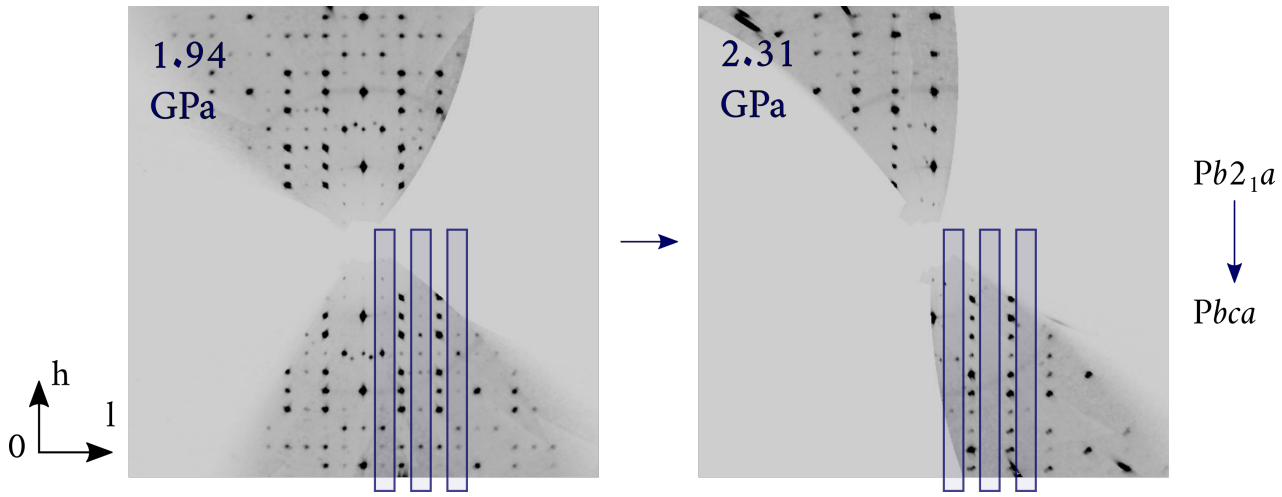

Figure S4.15: Second phase transition in quasi-hydrostatic medium analysis on layer *h0l* for series 4. Region where reflection from $\mathbf{c}_{[010]}$ glide plane should be extinct ($l = 2n + 1$) is framed. Lack of reflections in this region at 2.31 GPa confirms phase transformation P$b2_1a \rightarrow$ Pbca.

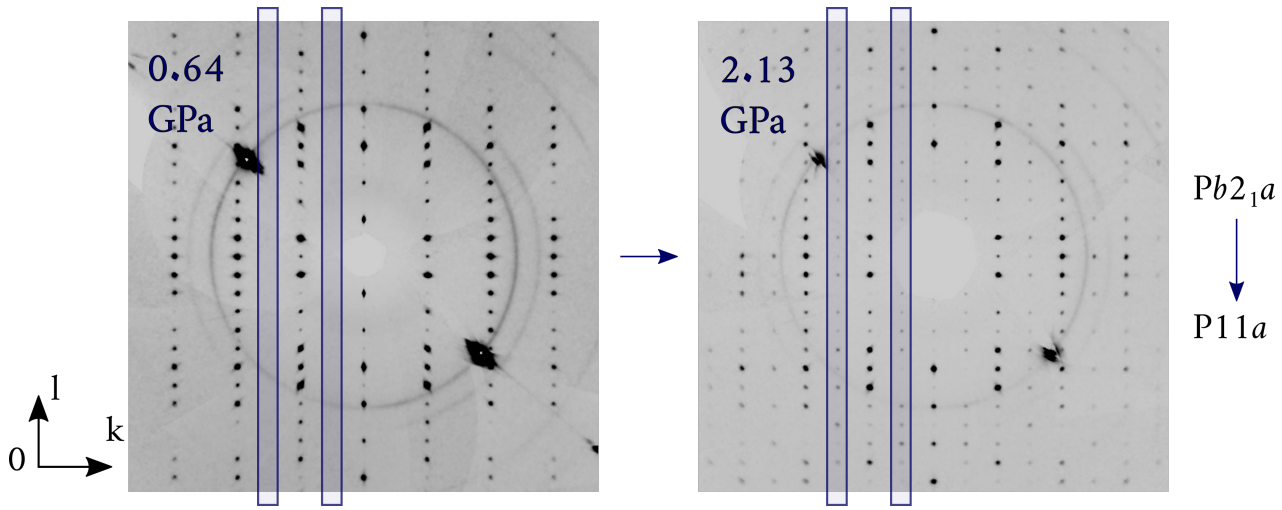

Figure S4.16: Second phase transition in non-hydrostatic medium analysis on layer *0kl* for series 3. Region where reflection from $\mathbf{b}_{[100]}$ glide plane should be extinct ($k = 2n + 1$) is framed. Lack of reflections in this region at 2.13 GPa confirms phase transformation P$b2_1a \rightarrow$ P11a.

S4.3 Second phase transition analysis

S4.3.1 *in-house* measurement

One data from *in-house* experiments for series 4 in quasi-hydrostatic medium turned out to be non-solvable both in P*bca* and P$b2_1a$ space groups, even with many constrains and restrains. Synchrotron measurements reveal that this may be data from pressure transition point. Second phase transition in quasi-hydrostatic medium has been confirmed by analysis of systematic extinctions on *h*0*l* layer. For *in-house* data at 2.16 GPa there are no systematic extinctions from $\mathbf{c}_{[010]}$ glide plane, what suggest P$b2_1a$ space group (Figure S4.17). However, number and intensity of reflections conflicting $\mathbf{c}_{[010]}$ glide plane is lower than those values at lower pressure (Table S4.16). As the result, data represents intermediate state, unfortunately in quality not suitable for further analysis.

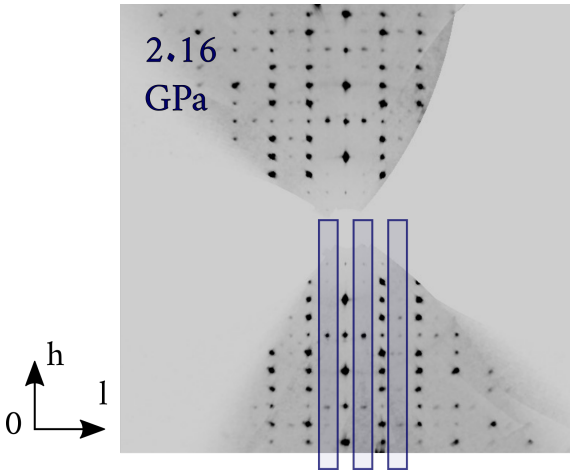

Figure S4.17: Layer *h*0*l* from *in-house* data at 2.16 GPa in quasi-hydrostatic medium. Region where reflection from $\mathbf{c}_{[010]}$ glide plane should be extincted ($l = 2n + 1$) is framed. Reflections in this region confirms that phase transformation P$b2_1a \rightarrow$ P*bca* didn't occur.

Table S4.16: Systematic absence expections for pressure points near 2.16 GPa for series 4 (appr6).

	b – –			– c –		
	1.94 GPa	2.16 GPa	2.31 GPa	1.94 GPa	2.16 GPa	2.31 GPa
N	178	171	160	431	407	241
N I>3s	0	0	1	231	121	18
<I>	0.2	0.3	0.2	10.4	2.2	0.9
<I/s>	0.2	0.2	0.2	5.1	2.0	0.9

S4.3.2 Synhrotron measurement

Notably, not all crystal specimens investigated at the synchrotron exhibited identical behavior. One crystal did not undergo a $Pb2_1a \rightarrow Pbca$ during the fast data collection series and displayed diffraction pattern indicative of higher symmetry only after further pressure increase (Figure 10).

S5 Script for distances calculations

To calculate distances between atoms in structures, Daniel Tchoń's script in Python [Tchoń(2024)] was modified and used. Searched distances were determined from crystal structure (Figure S5.18). Then symmetry operations leading to achieving chosen atoms from asymmetric unit were analyzed (Table S5.17). Before preparing script it is crucial to ensure, that all structures from one phase have exactly the same asymmetric unit and numeration of atoms.

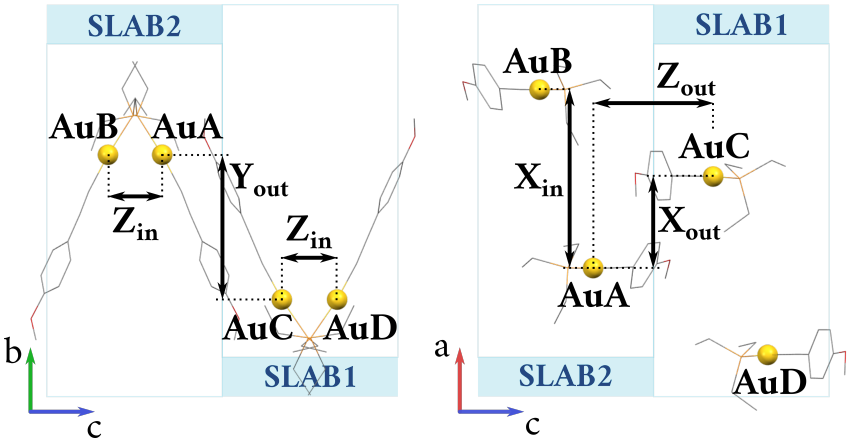

Figure S5.18: Definitions of distances inside and between SLABs with gold atoms names unification. Additionally, sum_{out} parameter was defined as summarized distance between atoms AUA and AuC. SLABs distinctions based on P$b2_1a$ space group. SLAB1 refers to molecules with conformation C, while SLAB2 – with conformation E of triethylphosphine moiety.

Table S5.17: Definitions of atoms AuA–AuD for all structures used in script. Symmetry operations for aryl moieties used in calculations were the same.

	AuA	AuB	AuC	AuD
P*bca*	Au1_(x, y, z)	Au1_(0.5+x, y, 0.5-z)	Au1_(1-x, 1-y, 1-z)	Au1_(0.5-x, 1-y, 0.5+z)
P$b2_1a$	Au1_(x, y, z)	Au1_(0.5+x, y, -z)	Au2_(x, y, z)	Au2_(-0.5+x, y, 1-z)
P11*a*	Au1_(x, y, z)	Au1_(0.5+x, y, 1-z)	Au4_(-0.5+x, -1+y, 1-z)	Au4_(x, -1+y, -1+z)
	Au3_(x, y, z)	Au3_(-0.5+x, y, 1-z)	Au2_(0.5+x y, 1-z)	Au2_(x, y, -1+z)

For this work, calculations between neighboring gold atoms, distances between centers of neighboring aryl rings and angle between ring plane and **a** direction in th unit cell were calculated. Results are shown on Figures S5.19 and S5.20.

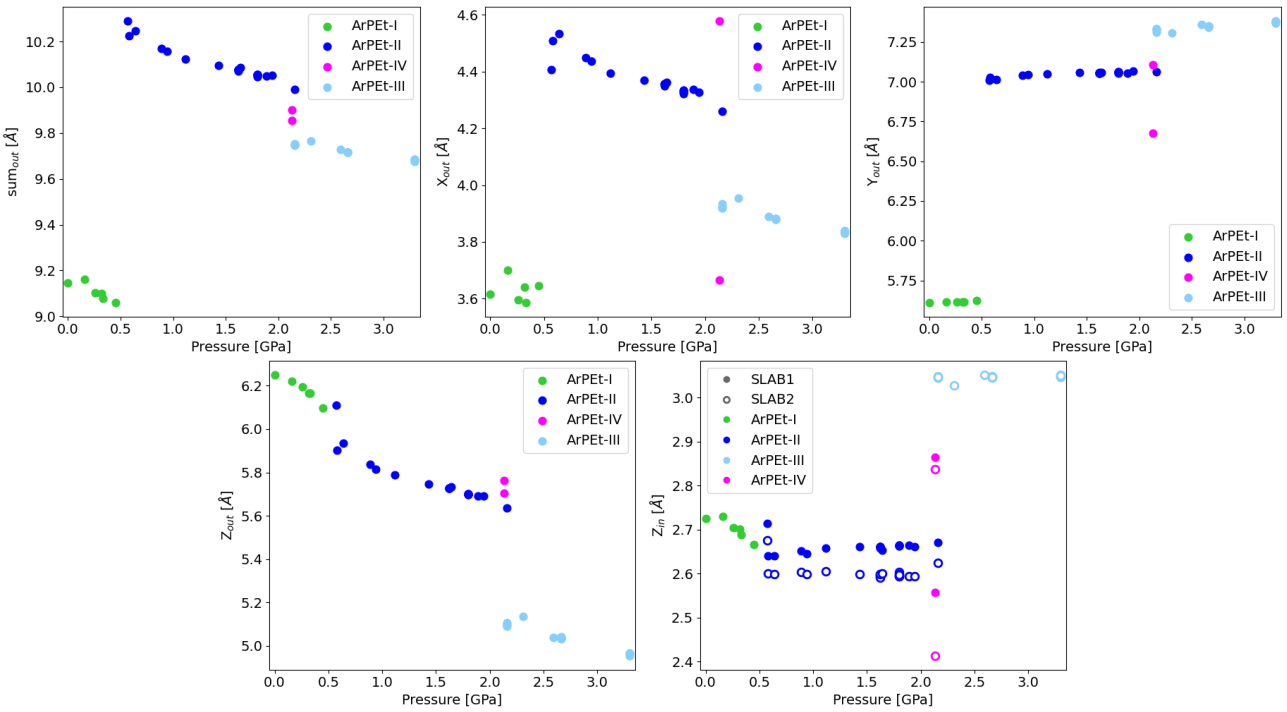

Figure S5.19: Calculated distances between neighboring gold atoms. Phases are distinguished by colors, while SLABs – by filling.

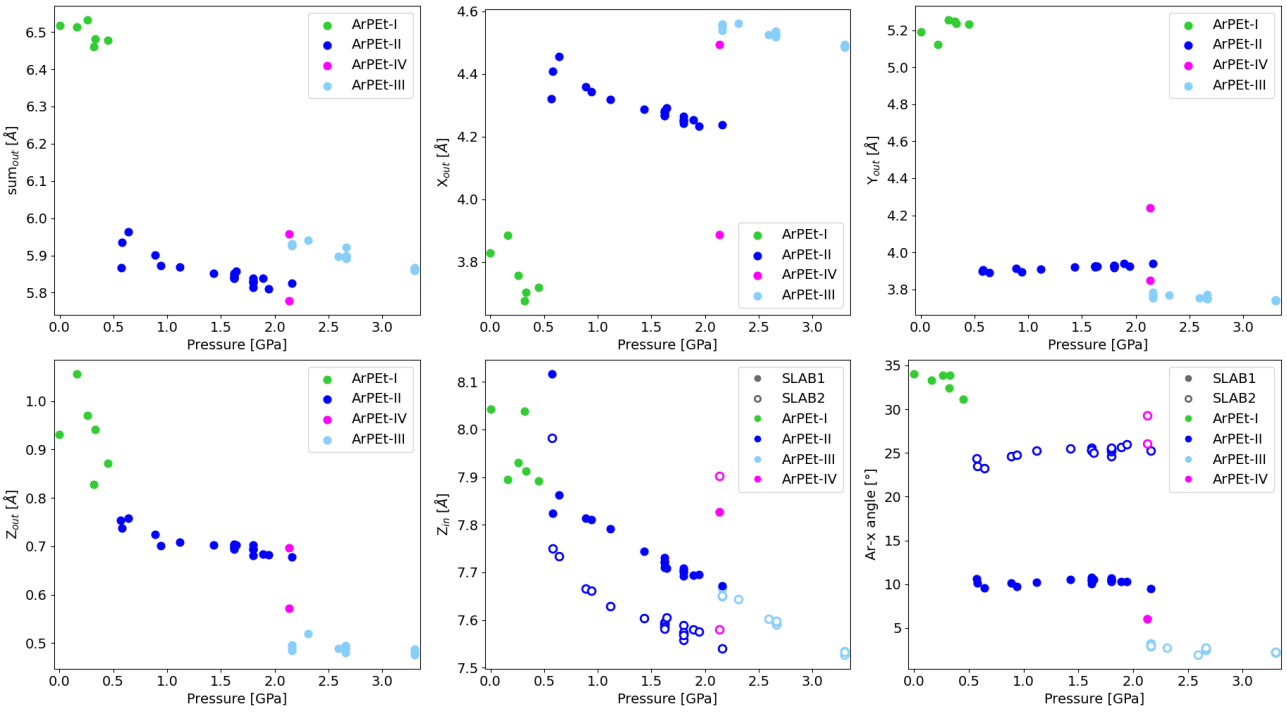

Figure S5.20: Calculated distances between neighboring gold aryl moieties and angle between aryl moieties and **a** direction in unit cell. Phases are distinguished by colors, while SLABs – by filling.

S6 Theoretical calculations

S6.1 Theoretical UV-vis spectrum of ArPEt in dichlorometane

Geometry of a single molecule of **ArPEt**, as taken from **ArPEt-I** crystal structure, was optimized using PCM approximation of the dichloromethane solvent in Gaussian16 [Frisch(2016)]. Calculations were performed using B3LYP/LANL2DZ method augmented with an empirical dispersion correction as proposed by Grimmme[Grimme *et al.*(2010)Grimme, Antony, Ehrlich, Electronic excitations were calculated using time-dependent DFT method (TD-DFT) [Adamo and Jacquemin(2013)]. *Ab-initio* predicted UV-vis spectrum in dichlorometane agrees qualitatively with experimental results predicting absorption maximum at about 293 nm. Frontier orbitals are presented in Figure S6.21. The predicted $S_0 \rightarrow S_1$ electronic excitation at 293 nm is essentially a Ligand to Metal charge transfer of $\pi \rightarrow \pi*$ type.

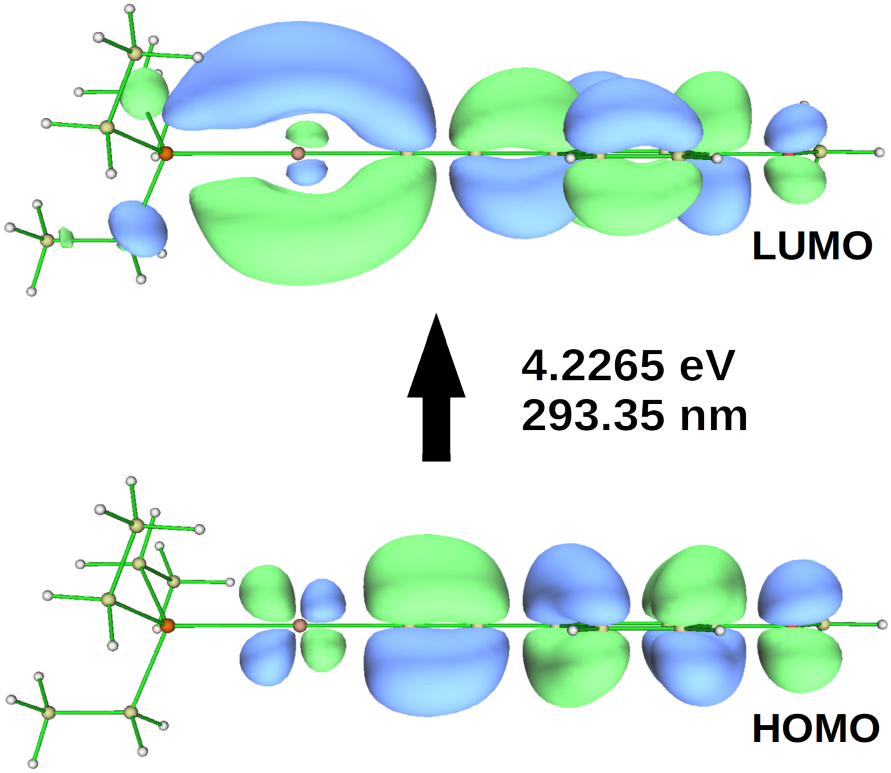

Figure S6.21: Representation of HOMO and LUMO frontier orbitals contributing to the $S_0 \rightarrow S_1$ electronic excitation visualized with MultiWFN [Lu and Chen(2012), Lu(2024)]; 0.025 e/Å^3 isosurfaces were used, blue - positive and green - negative.

S6.2 Optimization of ArPEt crystal structures

Symmetry of each **ArPEt** polymorph was maintained during the optimization process. External pressures were set for high-pressure crystal phases. A full relaxation of both lattice parameters and atomic coordinates by means of analytical energy gradients was applied when possible In the case of **ArPEt-II**, full relaxation of both lattice parameters and atomic coordinates did not converge within chosen strict criteria. Unit cell parameters obtained from XRD experiments differed from optimized ones by about 10%, for all **ArPEt** polymorphs. Cell volumes, obtained in last few cycles of not completely converged full relaxation of **ArPEt-II** don't differ one from another. Therefore, in the final optimization of lattice parameters and atomic coordinates of **ArPEt-II**, cell volume was constrained to the value from the former optimization.

The basis set, method and parameters used in the optimization of crystal structures, as well as, in the rest of theoretical calculations are listed in Table S6.18.

Table S6.18: Basis sets, method and parameters used in the theoretical calculations

Program	CRYSTAL17 [Dovesi(2017)]
Basis set: O, C, H,	6-31d1_gatti [Gatti *et al.*(1994)Gatti, Saunders, and Roetti]
Basis set: Au	Au_weihrich [Weihrich and Anusca(2006)]
Basis set: P	P_85-21d1G_zicovich [Zicovich-Wilson *et al.*(2002)Zicovich-Wilson, Bert, Roetti, Dovesi, and Saunders]
method	B3LYP-D* [Grimme *et al.*(2010)Grimme, Antony, Ehrlich, and Krieg] [Civalleri *et al.*(2008)Civalleri, Zicovich-Wilson, Valenzano, and Ugliengo]
Shrinking factor	8

S6.3 Theoretical estimation of Birch-Murnaghan's Equation of States - EOS

The variation of the crystal structures with pressure was theoretically simulated and fitted with the third-order Birch-Murnaghan's Equation of States (EOSs) using CRYSTAL17 computer code. Starting geometries and all the parameters used in the calculations are shown in Table S6.19.

Table S6.19: Parameters used to simulate theoretical EOS

EOS start geometry & Vopt	ArPEt-I	ArPEt-II	ArPEt-III
EOS pressure range	0 GPa - 2.6 GPa	0 GPa - 3.9 GPa	1.2 GPa- 4.5 GPa
EOS volume range	Vopt - 0.9Vopt	1.07Vopt - 0.9Vopt	1.025Vopt - 0.9325Vopt
EOS optimization steps	8	8	5

References

[Tchoń and Makal(2021)] D. Tchoń and A. Makal, *IUCrJ*, 2021, **8**, 1006–1017.

[Klotz *et al.*(2009)Klotz, Chervin, Munsch, and Le Marchand] S. Klotz, J.-C. Chervin, P. Munsch and G. Le Marchand, *Journal of Physics D: Applied Physics*, 2009, **42**, 075413.

[Angel *et al.*(2007)Angel, Bujak, Zhao, Gatta, and Jacobsen] R. J. Angel, M. Bujak, J. Zhao, G. D. Gatta and S. D. Jacobsen, *Journal of Applied Crystallography*, 2007, **40**, 26–32.

[Tchoń(2024)] D. Tchoń, *picometer, GitHub, https://github.com/Baharis/picometer*, 2024.

[Frisch(2016)] M. J. Frisch, *Gaussian˜16 Revision C.01*, 2016, G. W. Trucks and H. B. Schlegel and G. E. Scuseria and M. A. Robb and J. R. Cheeseman and G. Scalmani and V. Barone and G. A. Petersson and H. Nakatsuji and X. Li and M. Caricato and A. V. Marenich and J. Bloino and B. G. Janesko and R. Gomperts and B. Mennucci and H. P. Hratchian and J. V. Ortiz and A. F. Izmaylov and J. L. Sonnenberg and D. Williams-Young and F. Ding and F. Lipparini and F. Egidi and J. Goings and B. Peng and A. Petrone and T. Henderson and D. Ranasinghe and V. G. Zakrzewski and J. Gao and N. Rega and G. Zheng and W. Liang and M. Hada and M. Ehara and K. Toyota and R. Fukuda and J. Hasegawa and M. Ishida and T. Nakajima and Y. Honda and O. Kitao and H. Nakai and T. Vreven and K. Throssell and Montgomery, Jr., J. A. and J. E. Peralta and F. Ogliaro and M. J. Bearpark and J. J. Heyd and E. N. Brothers and K. N. Kudin and V. N. Staroverov and T. A. Keith and R. Kobayashi and J. Normand and K. Raghavachari and A. P. Rendell and J. C. Burant and S. S. Iyengar and J. Tomasi and M. Cossi and J. M. Millam and M. Klene and C. Adamo and R. Cammi and J. W. Ochterski and R. L. Martin and K. Morokuma and O. Farkas and J. B. Foresman and D. J. Fox.

[Grimme *et al.*(2010)Grimme, Antony, Ehrlich, and Krieg] S. Grimme, J. Antony, S. Ehrlich and H. Krieg, *The Journal of Chemical Physics*, 2010, **132**, 154104.

[Adamo and Jacquemin(2013)] C. Adamo and D. Jacquemin, *Chem. Soc. Rev.*, 2013, **42**, 845–856.

[Lu and Chen(2012)] T. Lu and F. Chen, *Journal of Computational Chemistry*, 2012, **33**, 580–592.

[Lu(2024)] T. Lu, *The Journal of Chemical Physics*, 2024, **161**, 082503.

[Dovesi(2017)] Dovesi, *Saunders, Roetti, Orlando, Zicovich-Wilson, Pascale, Doll, Harrison, Bush, D'Arco, Lunell, Causà, Noël, Maschio, Erba, Casassa, Rerat, Michel CRYSTAL17 User's Manual (University of Torino, Torino, 2017)*, 2017.

[Gatti *et al.*(1994)Gatti, Saunders, and Roetti] C. Gatti, V. R. Saunders and C. Roetti, *The Journal of Chemical Physics*, 1994, **101**, 10686–10696.

[Weihrich and Anusca(2006)] R. Weihrich and I. Anusca, *ChemInform*, 2006, **37**, year.

[Zicovich-Wilson *et al.*(2002)Zicovich-Wilson, Bert, Roetti, Dovesi, and Saunders] C. M. Zicovich-Wilson, A. Bert, C. Roetti, R. Dovesi and V. R. Saunders, *The Journal of Chemical Physics*, 2002, **116**, 1120–1127.

[Civalleri *et al.*(2008)Civalleri, Zicovich-Wilson, Valenzano, and Ugliengo] B. Civalleri, C. M. Zicovich-Wilson, L. Valenzano and P. Ugliengo, *CrystEngComm*, 2008, **10**, 405–410.